Journal of Cleaner Production 274 (2020) 122926

Contents lists available at ScienceDirect

Journal of Cleaner Production

journal homepage: www.elsevier.com/locate/jclepro

Hysteretic effects of meteorological conditions and their interactions on particulate matter in Chinese cities

Tuanhui Wang [a, b, 1], Hongquan Song [a, b, c, 1, *], Feng Wang [a, b], Shiyan Zhai [a, b], Zhigang Han [a, b], Dong Wang [d], Xiaoyang Li [a, b], Haipeng Zhao [a, b], Rui Ma [a, b], Guangli Zhang [a, b]

[a] *Laboratory of Geospatial Technology for the Middle and Lower Yellow River Regions (Henan University), Ministry of Education, Kaifeng, Henan, 475004, China*
[b] *Institute of Urban Big Data, College of Environment and Planning, Henan University, Kaifeng, Henan, 475004, China*
[c] *Henan Key Laboratory of Integrated Air Pollution Control and Ecological Security, Henan University, Kaifeng, Henan, 475004, China*
[d] *School of Life Sciences, Henan University, Kaifeng, Henan, 475004, China*

ARTICLE INFO

Article history:
Received 10 December 2019
Received in revised form
14 June 2020
Accepted 15 June 2020
Available online 18 July 2020

Handling editor. Cecilia Maria Villas Bôas de Almeida

Keywords:
Air pollution
$PM_{2.5}$
PM_{10}
GeoDetector
Lagged effects

ABSTRACT

Particulate matter (PM) has become the main air pollutant in most cities of in China, which greatly threatens the human health. Numerous studies have reported that PM concentrations could be accurately predicted from previous days' meteorological conditions. However, the hysteretic or lagged effects of meteorological factors on PM concentrations are not clear. In this study, the GeoDetector *q* statistic method was used to quantify the hysteretic influences of meteorological conditions and their interactions on concentrations of $PM_{2.5}$ (particles < 2.5 μm in aerodynamic diameter) and PM_{10} (particles < 10 μm in aerodynamic diameter) and the ratio of $PM_{2.5}$ to PM_{10} ($PM_{2.5}/PM_{10}$) at multiple spatial and temporal scales in China. We found that the temperature, precipitation, and relative humidity had primary impacts on $PM_{2.5}$ concentrations, PM_{10} concentrations, and the $PM_{2.5}/PM_{10}$ ratios, respectively, at both national and annual time scales. At the seasonal time scale, precipitation and relative humidity had hysteretic effects on PM concentrations in spring and summer, respectively. Moreover, precipitation and wind speed were dominant hysteretic factors in autumn and winter, respectively. At the regional scale, the dominant hysteretic effects of meteorological factors showed large variations across all regional subdivisions. The interactions between any two meteorological factors had an enhanced hysteretic effect on PM concentrations compared to a single factor. These findings could help us to develop scientific measures to reduce the emissions of air pollution and improve the performance of air pollution prediction models.

1. Introduction

Airborne particulate matter (PM), including $PM_{2.5}$ (particles smaller than 2.5 μm in aerodynamic diameter) and PM_{10} (particles smaller than 10 μm in aerodynamic diameter) is prone to accumulate harmful substances, such as heavy metals, polycyclic aromatic hydrocarbons, which can enter the respiratory system and have adverse effects on human health (Miranda et al., 2012; Liu et al., 2019). Numerous epidemiological studies have reported that long-term and short-term exposure to high PM concentrations are associated with increased morbidity, hospital admissions, and premature mortality (Aunan et al., 2018; Hong et al., 2019; Zhu et al., 2019; Xie et al., 2020). PM concentrations were far exceed the annual mean PM guideline of World Health Organization (WHO) ($PM_{2.5}$, 10 μg m^{-3}; PM_{10}, 20 μg m^{-3}) in all the 366 Chinese cities (Li et al., 2019b). Moreover, PM can scatter and absorb solar radiation, thereby directly reducing atmospheric visibility and impacting both the local climate and the local environment (Gu et al., 2010; Jing et al., 2020). Therefore, PM pollution has become a severe public health and environmental issue during recent years in China (Guan et al., 2019; Khan et al., 2019; Phosri et al., 2019), especially in regions of the North China Plain, eastern China, and

* Corresponding author. College of Environment and Planning, Henan University Jinming Campus, Kaifeng, Henan Province, 475004, China.
E-mail address: hqsong@henu.edu.cn (H. Song).
[1] These authors contributed equally to this work and should be considered co-first authors.

https://doi.org/10.1016/j.jclepro.2020.122926
0959-6526/

Abbreviations

PE	accumulated precipitation
PS	surface air pressure
RH	relative humidity at 2-m above the ground
SD	sunshine duration
TE	air temperature at 2-m above the ground
WS	wind speed
EC	eastern coastal area
MUPR	middle and upper reaches of the Pearl River
MUYR	middle and upper reaches of the Yangtze River
MYR	middle reaches of the Yellow River
NC	northern coastal area
NE	northeast area
QTP	Qinghai-Tibetan Plateau
SC	southeast coastal area
UYR	upper reaches of the Yellow River
XJ	Xinjiang

central China (Xue et al., 2019; Zhang et al., 2020).

Meteorological conditions and air pollutant emissions are the two main determinants of the ground level PM concentrations (Li et al., 2015a; Wang and Ogawa, 2015; Wang et al., 2015; He et al., 2017; Yang et al., 2018). To investigate the impacts of meteorological factors on PM concentrations, numerous studies have been conducted to analyze the correlations between them (Huang et al., 2015; Li et al., 2015b, 2019a, b; Chen et al., 2016; Yin et al., 2016; Miao et al., 2018). Generally, these studies indicated that precipitation and wind speed negatively correlate with PM concentrations (Wang and Ogawa, 2015; Wang et al., 2015; Wang et al., 2018; Chen et al., 2016; Li et al., 2019b). However, studies have shown great spatial and temporal variations in the correlations between concentrations of different sized PM and other meteorological factors, such as the relative humidity can enhance secondary PM conversion or PM wet deposition (Chen et al., 2017; Kliengchuay et al., 2018), air temperature/sunshine duration would strengthen the dispersion condition or stimulate the PM conversion (Chen et al., 2017; Miao et al., 2018; Li et al., 2019a, 2019b; Zhang et al., 2019), and surface atmospheric pressure can directly affect the wind speeds and then the PM transport (Li et al., 2015b, 2017a, 2019b, 2017b). Moreover, previous studies have also shown that East Asian winter winds play an important role in the PM transport (Wang et al., 2019).

The above-mentioned studies have comprehensively explored correlations between PM concentrations and meteorological factors, but they mainly concentrated on PM and meteorological conditions on a single day with a limited number of locations and short time frames. Several studies have shown that PM concentrations may be influenced by prior days' meteorological conditions (Hien et al., 2002; Ito et al., 2007; Zhang et al., 2013; Huang et al., 2015; Guo et al., 2016; Chen et al., 2018a, 2018b). The previous days' precipitation also has significant impacts on PM_{10} concentrations; for example, rainfall on one day can remove PM from the air, thereby reducing PM concentrations on the following days (Hien et al., 2002; Barmpadimos et al., 2011; Song et al., 2017). This converts the air pollutant emissions problem into a wet deposition/acid rain problem, leading to subsequent adverse effects on vegetation, soil quality, ecosystems, surface water, etc. (Huang et al., 2009; Shen et al., 2013; Huang et al., 2020). Although hysteretic effects of meteorological conditions on PM are recognized as one of the crucial mechanisms of PM and some PM prediction models have considered previous days' meteorological variables to be input parameters (Chen et al., 2018b), few studies have quantified these effects.

To quantify the hysteretic effects of meteorological factors on PM, this study adopted the geographical detector q statistic method (GeoDetector) (Wang et al., 2010, 2016b), a spatial heterogeneity detector model, to analyze the effects of meteorological conditions on the next three days' concentrations of $PM_{2.5}$ and PM_{10} and the ratio of $PM_{2.5}$ to PM_{10} ($PM_{2.5}/PM_{10}$) in Chinese cities at multiple spatial and temporal scales. Study results could help us to better understand the relative importance of meteorological factors in the hysteretic effects on PM. More specifically, study results can provide knowledge needed to enhance the performance of air quality prediction models and to help the regional/local air quality management departments to develop reasonable control strategies. For example, the regional/local departments can determine the air pollutant emission reduction plan according to the weather conditions of the day to reduce PM pollution in the next few days in regions with severe PM pollutions.

2. Materials and methods

2.1. Datasets

This study concentrated on the hysteretic effects of meteorological factors on concentrations of $PM_{2.5}$ and PM_{10} and $PM_{2.5}/PM_{10}$ ratios in cities of mainland China. Hourly and daily observations of $PM_{2.5}$ and PM_{10} from January 1, 2015 to December 31, 2017 at 1497 air quality monitoring sites in 366 cities were obtained from the China National Environmental Monitoring Center (Fig. 1). The meteorological data at 839 stations from January 1, 2015 to December 31, 2017 were obtained from the China Meteorological Data Network (http://data.cma.cn) (Fig. 1), including accumulated precipitation (PE, mm), air temperature at 2-m above the ground (TE, °C), relative humidity at 2-m above the ground (RH, %), sunshine duration (SD, h), surface air pressure (PS, hPa), and wind speed at 10-m above the ground (WS, m s^{-1}).

The air quality monitoring sites and meteorological observation stations were not always at the same physical location (Fig. 1). It was necessary to match the location of meteorological and PM data for investigating the hysteretic effects of meteorological conditions on PM. The kriging interpolation method was adopted to generate the surface of meteorological factors using ArcMap 10.5 software (Esri: http://www.esri.com) based on the meteorological data at 839 monitoring stations. Then the six meteorological parameters were extracted from the kriged surfaces at the locations of the 366 cities in China. The evaluation of the kriging interpolation results (Li et al., 2019b) showed that this method has good predictive ability for meteorological factors based on observation data in China.

To comprehensively explore the spatial and temporal variations in hysteretic effects of meteorological factors on PM concentrations or $PM_{2.5}/PM_{10}$ ratios, we conducted analyses at multiple spatial and temporal scales. This study divided mainland China into ten regions on the basis of economic development, climate, and topography (Li et al., 2019b). They are EC (eastern coastal area), MUPR (middle and upper reaches of the Pearl River), MUYR (middle and upper reaches of the Yangtze River), MYR (middle reaches of the Yellow River), NC (northern coastal area), NE (northeast area), QTP (Qinghai-Tibetan Plateau), SC (southeast coastal area), UYR (upper reaches of the Yellow River), and XJ (Xinjiang). Please refer to Li et al. (2019b) for details as to how the regions are defined (Fig. S1). The whole year was divided into spring (March, April, and May), summer (June, July, and August), autumn (September, October, and November), and winter (December, January, and February). Figs. S2–S7 show the spatial distributions of seasonal meteorological conditions in China during 2015–2017 (Li et al., 2019b).

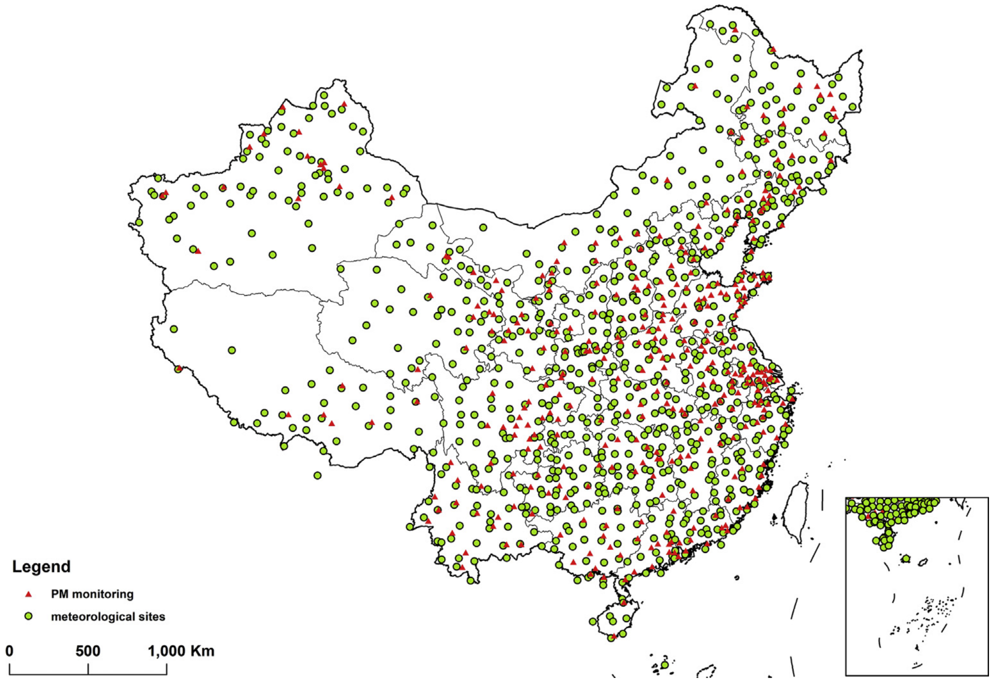

Fig. 1. Map of air quality monitoring stations and meteorological observation sites.

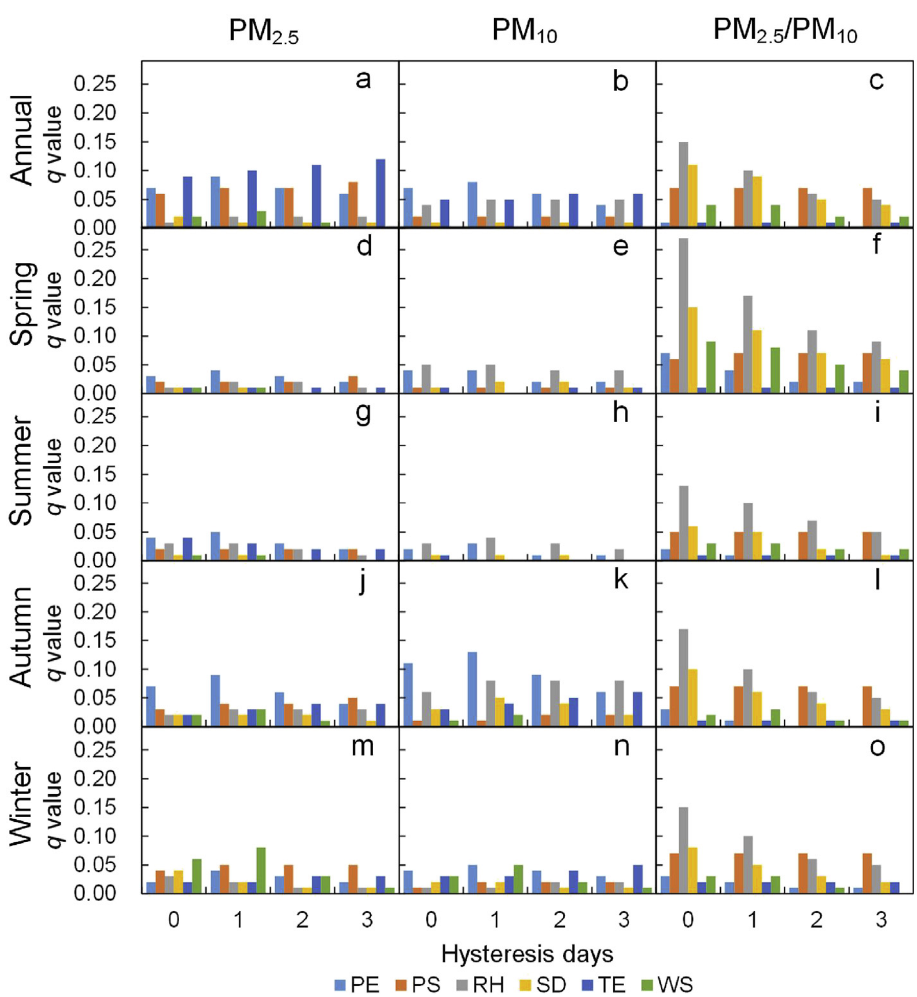

Fig. 2. Hysteretic effects of meteorological factors on concentrations of $PM_{2.5}$ (a, d, g, j, and m) and PM_{10} (b, e, h, k, and n) and $PM_{2.5}/PM_{10}$ (c, f, i, l, and o) at annual and seasonal time scales in China.

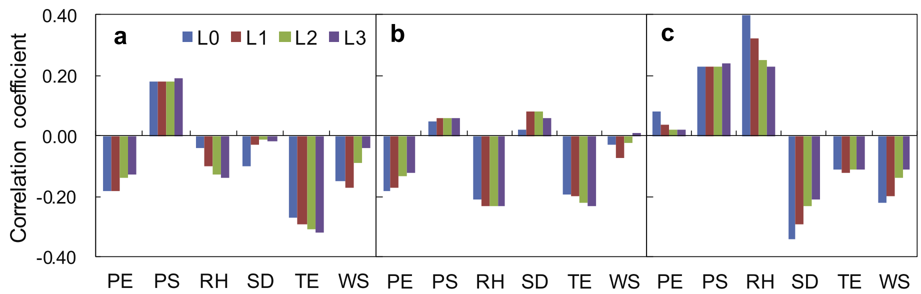

Fig. 3. Correlation coefficients between meteorological factors and concentrations of $PM_{2.5}$ (a) and PM_{10} (b) and $PM_{2.5}/PM_{10}$ ratios (c) of the next three days (lagged zero day, L0; lagged one day, L1; lagged two days, L2; lagged three days, L3).

2.2. GeoDetector q statistic

The GeoDetector q statistic was adopted to quantify the hysteretic effects of meteorological factors and their interactions on PM concentrations or the $PM_{2.5}/PM_{10}$ ratio in China. The GeoDetector q statistic is a spatial variance analysis model that assess non-linear associations between potential impacting factors (independent variables) and target geographic phenomenon (dependent variables) (Wang et al., 2010, 2016b). The underlying assumption of this model is that if X causes Y, then their spatial distributions will be consistent. Compared with traditional linear methods, GeoDetector q statistic has the ability of handling categories of dependent variables, detecting the relative importance of impacting factors, and investigating the interactive effect(s) between two X variables on Y. There is no need to consider whether there is a linear relationship between these two factors and to deal with collinearity between factors due to this method is immune to collinearity.

The spatial association between X (e.g. meteorological factors in this study) and Y (e.g. PM concentrations or $PM_{2.5}/PM_{10}$ ratios in this study) can be measured by the q value:

$$q = 1 - \frac{\sum_{h=1}^{L} N_h \sigma_h^2}{N\sigma^2} = 1 - \frac{SSW}{SST} \tag{1}$$

where $SSW = \sum_{h=1}^{L} N_h \sigma_h^2$, $SST = N\sigma^2$;

$h = 1, \ldots, L$ denotes the categories of X;
N_h: the count of samples in category h;
N: the total number of samples across the whole study area;
SSW: the sum of variance in category h in the study region;
SST: the sum of global variance in category h in the study region;
σ_h^2: the variances of samples in the category h;
σ^2: the global variance of Y.

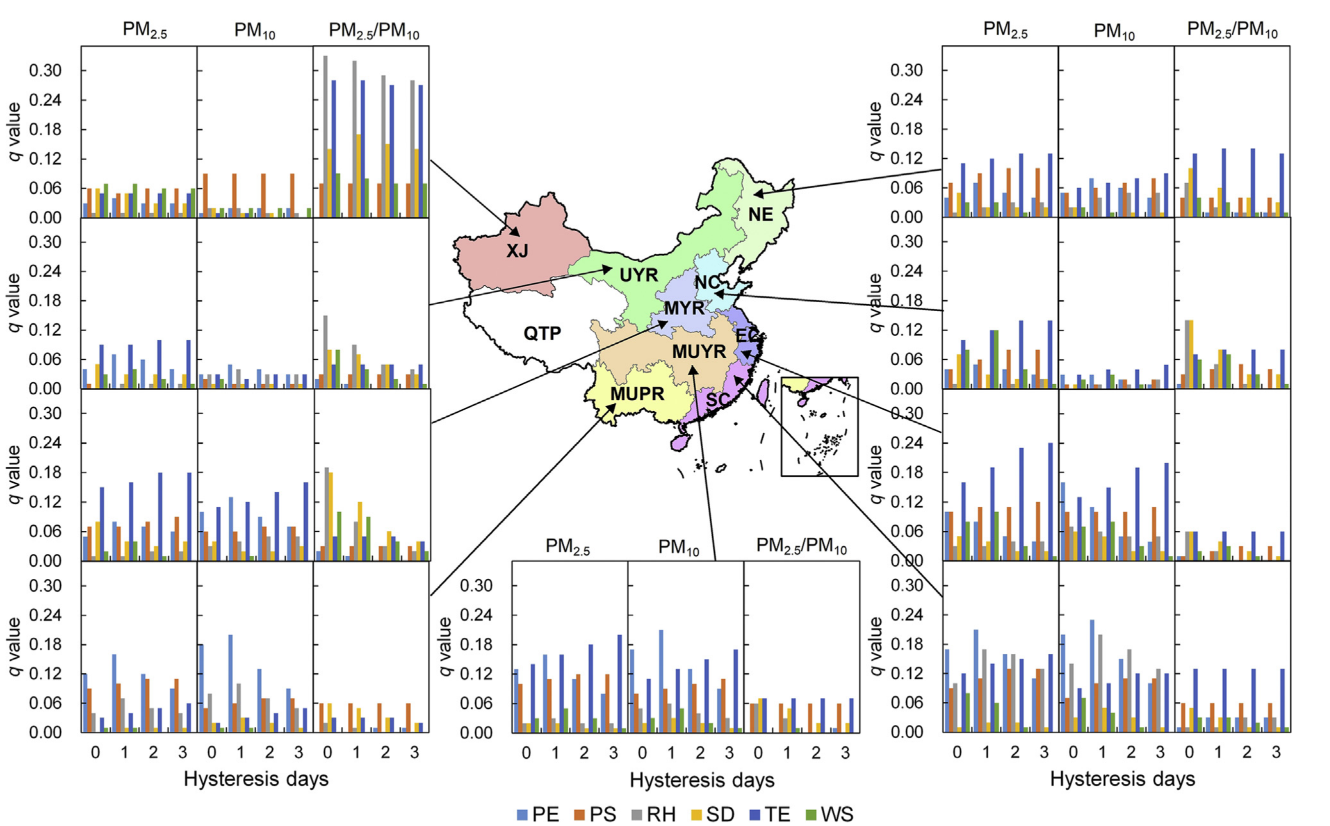

Fig. 4. Regional hysteretic effects of meteorological factors on particulate matter in China.

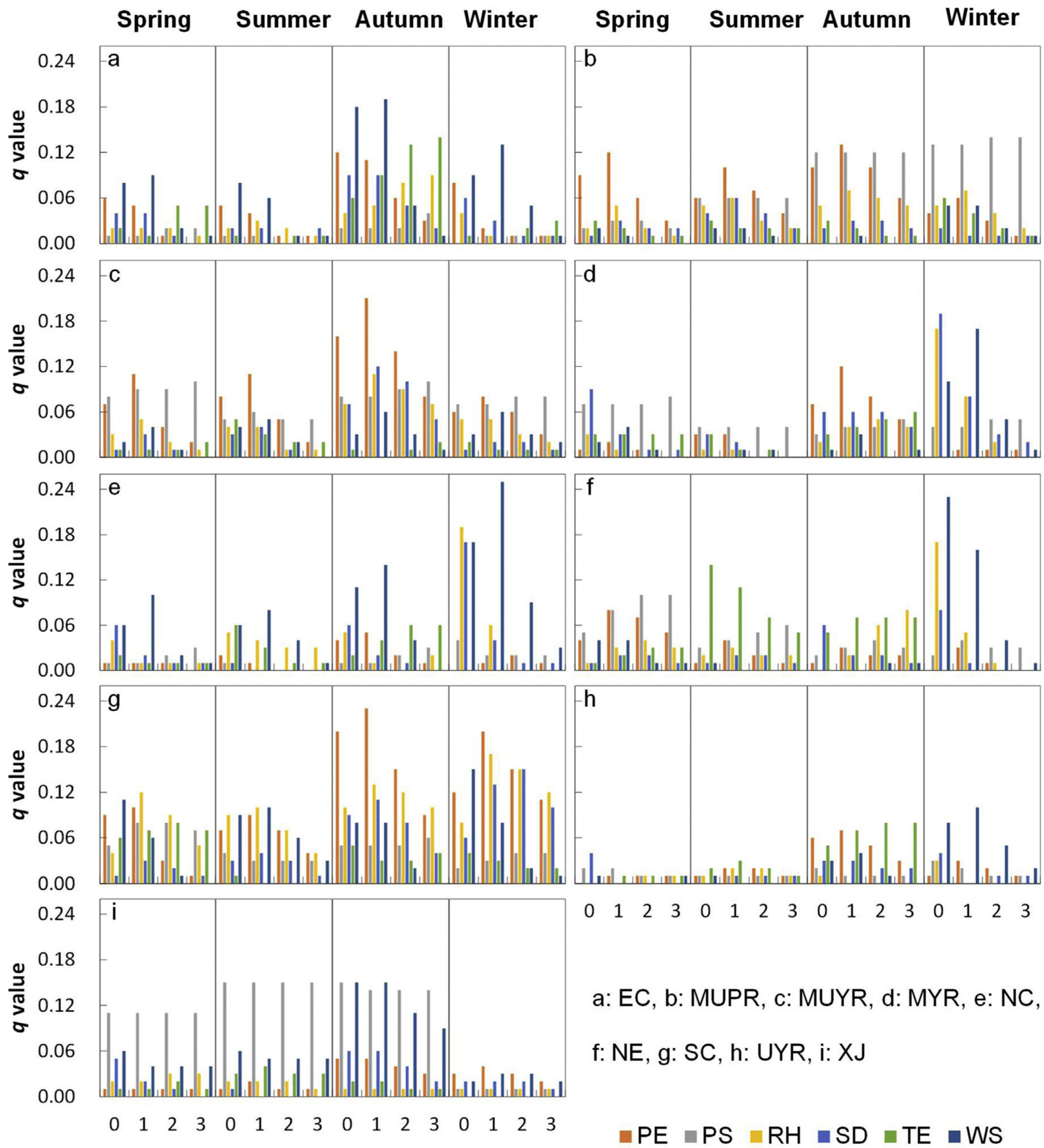

Fig. 5. Regional hysteretic effects of meteorological conditions on $PM_{2.5}$ in China.

The interval of q is [0, 1], indicating that X explains $q \times 100\%$ of PM concentrations or $PM_{2.5}/PM_{10}$ ratios. The greater the q value, the stronger the explanatory power of the meteorological factor to PM concentrations or $PM_{2.5}/PM_{10}$ ratios.

The GeoDetector q statistic model can also quantify effects of interactions between two X factors on PM concentrations or $PM_{2.5}/PM_{10}$ ratios. This index can be used to assess the interactive effects of two X variables by comparing the q values of two X variables with the q of a single X variable. The types of interaction possible between two X variables are described in Wang et al. (2016b).

3. Results

3.1. Effects on PM at the national scale

Fig. 2 shows the impacts of meteorological conditions on particulate matter at the nationwide scale. TE showed dominant hysteretic impacts on $PM_{2.5}$ concentrations at the annual time scale (Fig. 2a, Table S1). PE had strong impacts on PM_{10} concentrations on the same day (lagged day 0, L0) and one day later (lagged day 1, L1) (Fig. 2b). However, RH had strongest impacts on $PM_{2.5}/PM_{10}$ ratios of L0 and L1, followed by SD (Fig. 2c). To present PM was positive or negative correlated with hysteretic factors, we calculated the correlation coefficients between PM and meteorological factors during the following 3 day at multiple spatial and temporal scales (Fig. 3, S8-S13).

The hysteretic effects of meteorological conditions on PM showed seasonal variations in China (Fig. 2, Table S2), especially for $PM_{2.5}/PM_{10}$ ratios. PE was the major hysteretic factor of $PM_{2.5}$ on days of L1 and L2 (i.e, two days later, or lagged day 2) in spring and summer (Fig. 2d and g). RH had primary hysteretic effects on PM_{10} in spring and summer, followed by PE (Fig. 2e and h). In autumn, the primary hysteretic factor impacting $PM_{2.5}$ and PM_{10} was PE on days of L0, L1, and L2 (Fig. 2j and k). However, in winter, the dominant hysteretic factor of $PM_{2.5}$ was WS. RH had strongest hysteretic effects on $PM_{2.5}/PM_{10}$ ratios, and the influence decreased from L0 to L3 (i.e, three days later, or lagged day 3) in spring (Fig. 2f). Similar to spring, RH was the main hysteretic factor affecting $PM_{2.5}/$

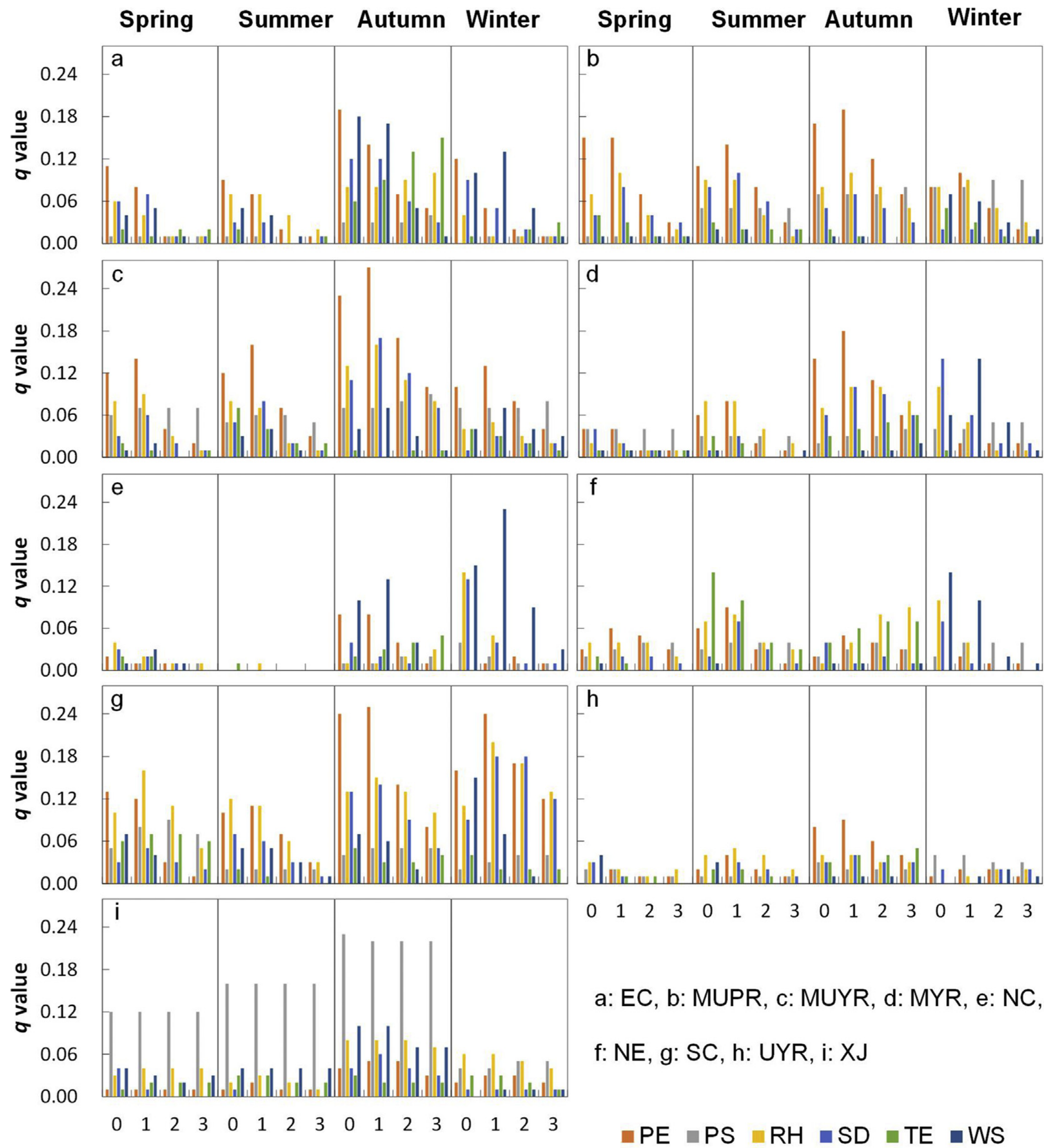

Fig. 6. Regional hysteretic effects of meteorological conditions on PM_{10} in China.

PM_{10} ratios in the other three seasons on days of L0 and L1 (Fig. 2i, l, and o), but the influence was weaker than in spring.

3.2. Regional effects on PM at the annual time scale

This study analyzed data from nine regions; QTP was not included due to its lower PM concentrations. There were significant regional variations in the hysteretic effects of meteorological conditions on PM at the annual time scale (Fig. 4, Table S3). In regions of EC, MUYR, MYR, NC, NE, and UYR, TE had the largest hysteretic effects on $PM_{2.5}$, while in the regions of MUPR and SC, PE was the dominant hysteretic factor. WS and PE also had significant effects on $PM_{2.5}$ concentrations on both L0 and L1 days in regions of NC and MUYR, respectively. For PM_{10}, the dominant hysteretic factor was PE in MUPR region. PE was the dominant impacting factor on L0 in EC region, but then it was TE. In regions of MUYR and MYR, PE was primary impacting factor of PM_{10} on L0 and L1, then the dominant factor was TE. PE was the primary influencing factor of PM_{10} on days of L0 and L1 in SC region, then it was RH. However, the meteorological conditions had no obvious hysteretic effects on PM_{10} concentrations in the regions of NC, NE, and UYR.

For $PM_{2.5}/PM_{10}$ ratios, TE was the primary hysteretic factor in regions of NE and SC, but RH was the primary hysteretic factor in UYR. In the region of MYR, RH was the dominant impacting factor of L0's $PM_{2.5}/PM_{10}$ ratios, but then SD was the hysteretic factor. RH and SD were approximately the same primary impacting factor of L0 day in NC region, then SD/TE on L1 and TE on days of L2 and L3. In XJ, however, RH and the closely followed TE were dominant hysteretic factors of $PM_{2.5}/PM_{10}$ ratios, followed by SD. In most regions, SD was the second most important factor, which relates to the secondary PM.

3.3. Regional effects on PM at seasonal time scale

Figs. 5–7 show that there were also large and significant seasonal variations in the hysteretic effects of meteorological

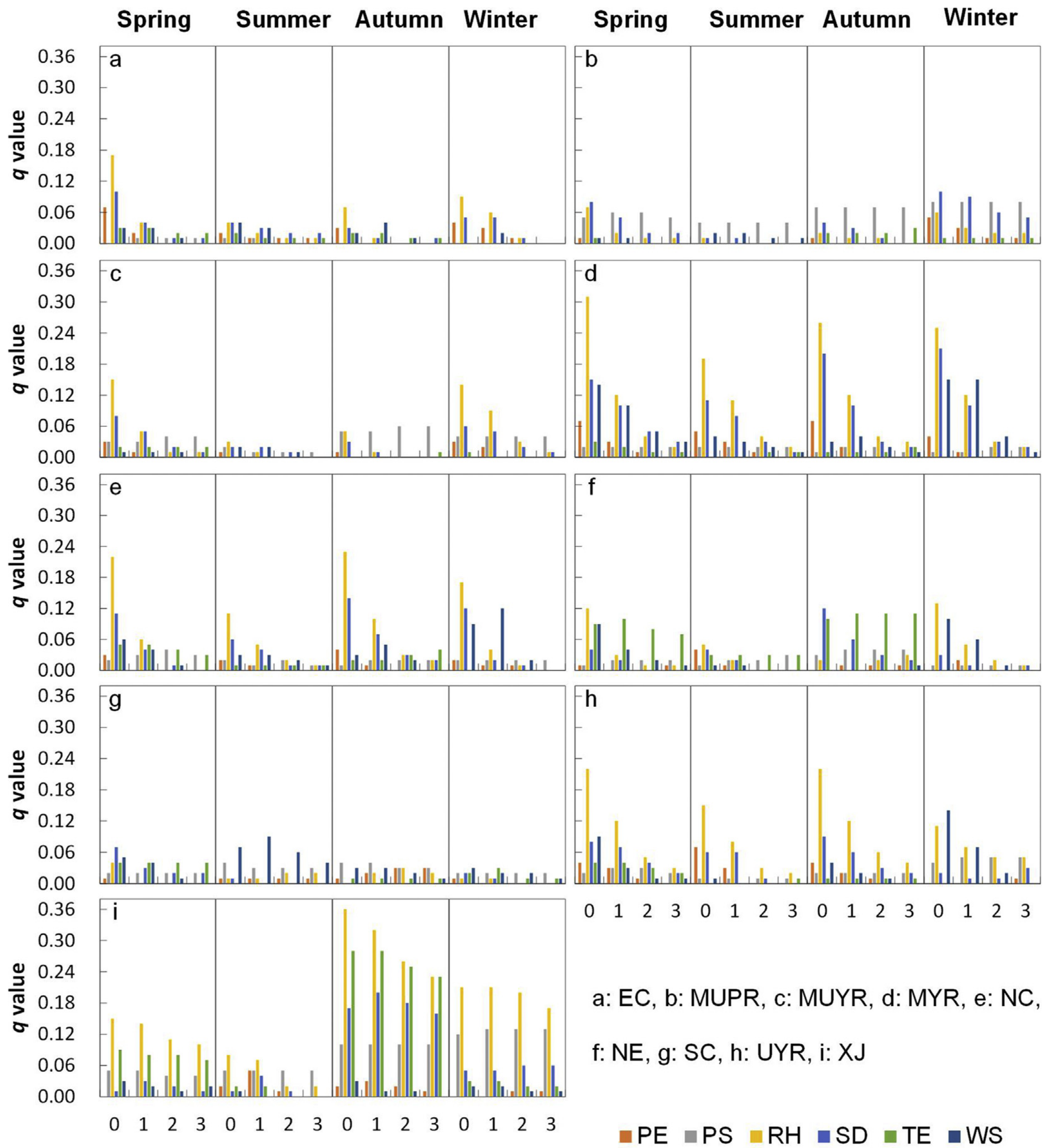

Fig. 7. Regional hysteretic effects of meteorological conditions on $PM_{2.5}/PM_{10}$ ratio in China.

conditions on PM over the nine regions at the seasonal time scale. In spring, PE was the dominant hysteretic factor of $PM_{2.5}$ in MUPR region, but the primary impacting factor was WS in regions of NC and EC (Fig. 5). In MUYR region, PE was the dominant factor of $PM_{2.5}$ on L1, then PS was the primary factor on days of L2 and L3. In regions of EC and MUPR, however, PE was the dominant impacting factor of PM_{10} in spring. PE was the major influencing factor of PM_{10} on days L0 and L1, then it was PS on days of L2 and L3. In SC region, however, PE was the dominant factor on L0, but then it was RH on days of L1 and L2. For $PM_{2.5}/PM_{10}$ ratios, RH was the major hysteretic factor in most regions of China except for MUPR and SC.

In summer, PE had significant hysteretic effects on concentrations of $PM_{2.5}$ and PM_{10} in MUPR and MUYR (Figs. 5–6). In SC region, SD, RH, and PE were the three main factors that affected $PM_{2.5}$ during L0-L3, but PE and RH were main impacting factors of PM_{10}. For $PM_{2.5}/PM_{10}$ ratios, RH and WS were dominant hysteretic factors in regions of MYR and UYR and in SC, respectively.

In autumn, however, WS and PE were the primary hysteretic factor of PM concentrations in regions of NC and EC and regions of MUYR, MYR, and SC, respectively. In MUPR, PS was the primary factor of $PM_{2.5}$ on days of L0, L2, and L3, but PE was main impacting factor on L1 day. However, PE was the dominant impacting factor of PM_{10} in MUPR. RH was the main hysteretic factor of $PM_{2.5}/PM_{10}$ ratios in regions of XJ, UYR, and MYR during L0-L3 and in NC on days of L0 and L1, but the principal factor was TE in NE.

In winter, WS was the leading factor of $PM_{2.5}$ and PM_{10} concentrations in regions of EC, NC, and NE, but the primary factor was PE on days of L0 and L1 and then was SD (L2) and RH (L3) in SC region. In MYR, SD was the dominant factor of $PM_{2.5}$ and PM_{10} on days of L0 and L1 (Figs. 5–6). WS and RH showed major hysteretic effects on $PM_{2.5}/PM_{10}$ ratios in regions of MYR, NC, NE, and UYR and in regions of EC, MUYR, and XJ, respectively. Moreover, PS was the principal hysteretic factor of PM concentrations in XJ during spring, summer, and autumn.

3.4. Interactive effects on PM at the national scale

There were 15 pairs of interactions between the six meteorological factors adopted in this study (we only listed the top 10 interaction *q* values in Figs. 8–10 due to the limited space). As

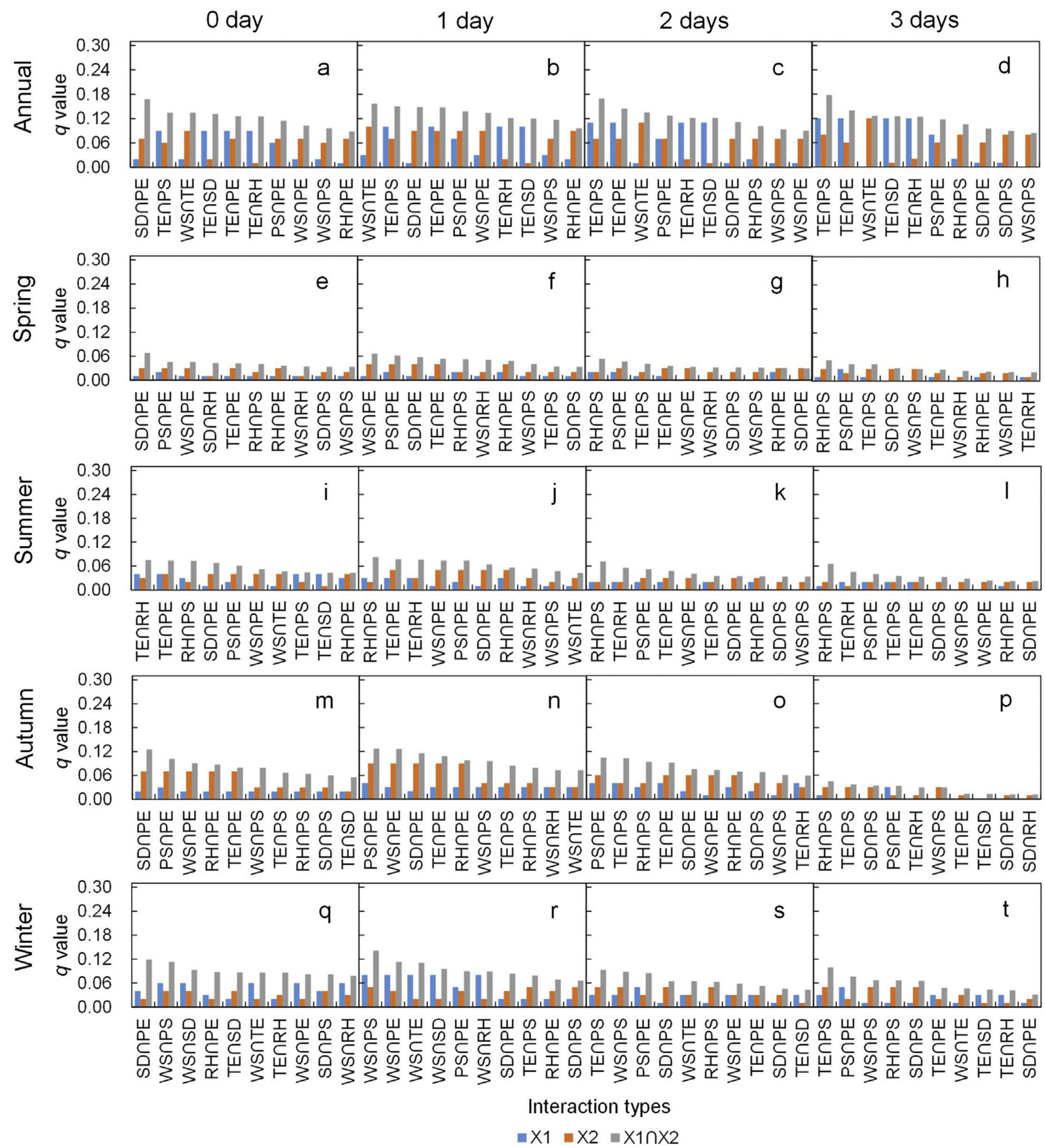

Fig. 8. Interactive hysteretic effects of meteorological conditions on $PM_{2.5}$ in China. The x-axis label X1∩X2 denotes q values of X1 (blue), X2 (yellow), and the interaction between X1 and X2 (grey). (For interpretation of the references to color in this figure legend, the reader is referred to the Web version of this article.)

shown in Fig. 8a–d, the interactions of SD∩PE (the '∩' symbol denotes the interaction between two *X* variables such as SD and PE), WS∩TE, and TE∩PS had strongest enhanced effects on $PM_{2.5}$ on days of L0, L1, and L2 and L3, respectively, at the national scale throughout the whole year, but there were no obvious effects on PM_{10} concentrations. The TE∩RH showed largest effects on $PM_{2.5}$/PM_{10} ratios during days of L0 and L1, but the strongest interactive effect was RH∩PS on days of L2 and L3.

Although interactions between meteorological factors showed enhanced effects on PM concentrations in spring and summer, these interaction *q* values were relative low compared to other seasons (Figs. 8–9). In spring, SD∩PE and WS∩PE showed largest effects on $PM_{2.5}$ on L0 and L1 (Fig. 8), respectively, but for PM_{10} they were SD∩RH and RH∩PS (Fig. 9). In summer, TE∩RH and RH∩PS had strongest effects on $PM_{2.5}$ on days of L0 and L1 (Fig. 8), respectively, but for PM_{10} it was TE∩RH (Fig. 9). RH∩PS showed biggest influence on both $PM_{2.5}$ and PM_{10} on days of L2 and L3. In autumn, PS∩PE and TE∩PE showed strongest effects on concentrations of $PM_{2.5}$ and PM_{10}, respectively, during days of L1 and L2 (Figs. 8–9). For the $PM_{2.5}$/PM_{10} ratio, the largest hysteretic interaction was RH∩PS on days of L1 and L2 during all four seasons (Fig. 10).

3.5. Interactive effects on PM at the regional scale

Fig. 11 shows the largest interaction *q* values between meteorological factors on each day in nine regions in China at the annual time scale (refer to Figs. S14–S16 for more information). In regions of NC and UYR, WS∩TE had significant impacts on the following three days' $PM_{2.5}$ concentrations (Fig. 11). However, WS∩TE and TE∩PS played important roles in $PM_{2.5}$ concentrations on day L1 and on days L2 and L3, respectively, in regions of MYR and NE (Fig. 11). In MUYR, TE∩PE showed significant impacts on L0-L2 days' $PM_{2.5}$ concentrations, but the interaction between TE and PS had great hysteretic effects on $PM_{2.5}$ on day L3 (Fig. 11). However, WS∩PE and TE∩PE had largest impacts on $PM_{2.5}$ on L0 and L1-L2, respectively, in SC region (Fig. 11). In regions of MUYR, MYR, and NE,

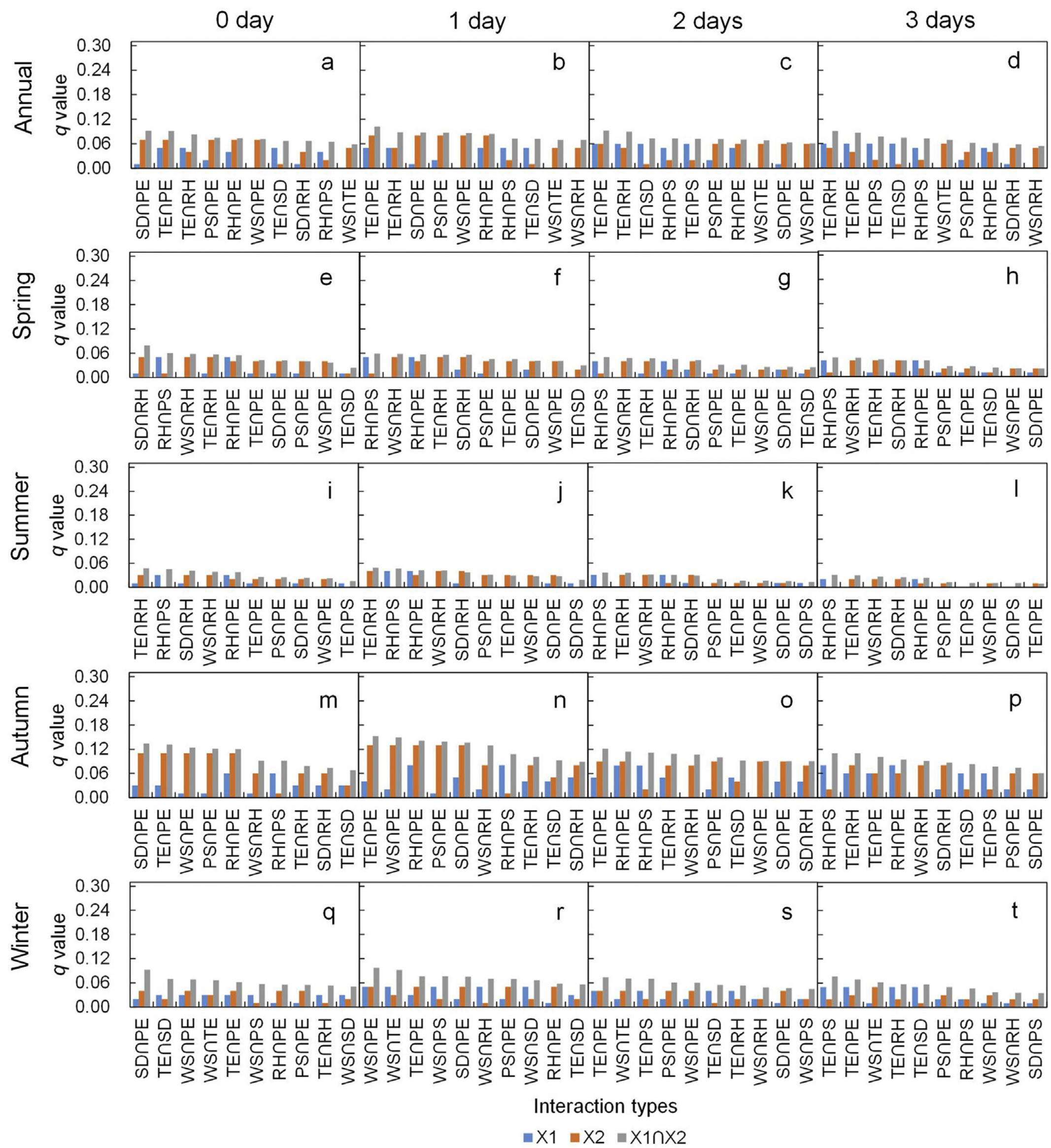

Fig. 9. Interactive hysteretic effects of meteorological conditions on PM_{10} in China. The x-axis label X1∩X2 denotes q values of X1 (blue), X2 (yellow), and the interaction between X1 and X2 (grey). (For interpretation of the references to color in this figure legend, the reader is referred to the Web version of this article.)

TE∩PE and TE∩PS had great impacts on PM_{10} concentrations on days of L1, L2, and L3. For $PM_{2.5}/PM_{10}$ ratios, the major hysteretic interaction was TE∩RH in regions of MUYR, NE, and NC on days of L0 and L1 and in regions of UYR and XJ on all days (Fig. 11). In addition, TE∩PS and WS∩TE were largest interactive effects on $PM_{2.5}$ and PM_{10} in EC and MUPR, respectively. In XJ region, PS∩PE was the main interaction affecting $PM_{2.5}$ and PM_{10} (Fig. 11).

Figs. S17–S28 show the regional hysteretic effects of interactions between meteorological factors on PM concentrations or $PM_{2.5}/PM_{10}$ ratios at the seasonal time scale, indicating that there were large seasonal and regional variations in the interactive effects of meteorological factors on PM in China. We mainly focused on analyzing interactions in regions of EC, MUYR, MYR, and NC in winter because PM pollution are severe in these regions in winter. RH∩PE and WS∩PE had largest impacts on $PM_{2.5}$ and PM_{10}, respectively, on L0 day in EC. However, WS∩SD and WS∩TE were the strongest interactive effects on PM concentrations on days of L1 and L2, respectively. For $PM_{2.5}/PM_{10}$ ratios, RH∩PS was the largest interaction on days of L0-L2. In NC region, WS∩RH showed greatest impacts on both PM concentrations and $PM_{2.5}/PM_{10}$ ratios on L0 day, then it was WS∩PS on days of L1 and L2 (Figs. S26–S28). In MUYR, PS∩PE was the strongest interaction impacting concentrations of $PM_{2.5}$ and PM_{10} on days of L0, L1, and L2, but it was RH∩PS for $PM_{2.5}/PM_{10}$ ratios (Fig. S27). In MYR, WS∩SD had strongest impacts on $PM_{2.5}$ on days of L0 and L1 (Fig. S26), but it was SD∩PE on L0 and WS∩PS on L1-L2 for PM_{10} (Fig. S27). For $PM_{2.5}/PM_{10}$, WS∩RH and WS∩SD showed largest influence on L0 and L1, respectively (Fig. S28).

4. Discussion

4.1. Hysteretic effects of meteorological factors

This study is the first comprehensive work, to the best of our knowledge, to quantify the hysteretic effects of meteorological factors and their interactions on PM concentrations or $PM_{2.5}/PM_{10}$ ratios at multiple spatial and temporal scales. We found that there were large spatial and seasonal variations in the hysteretic effects of

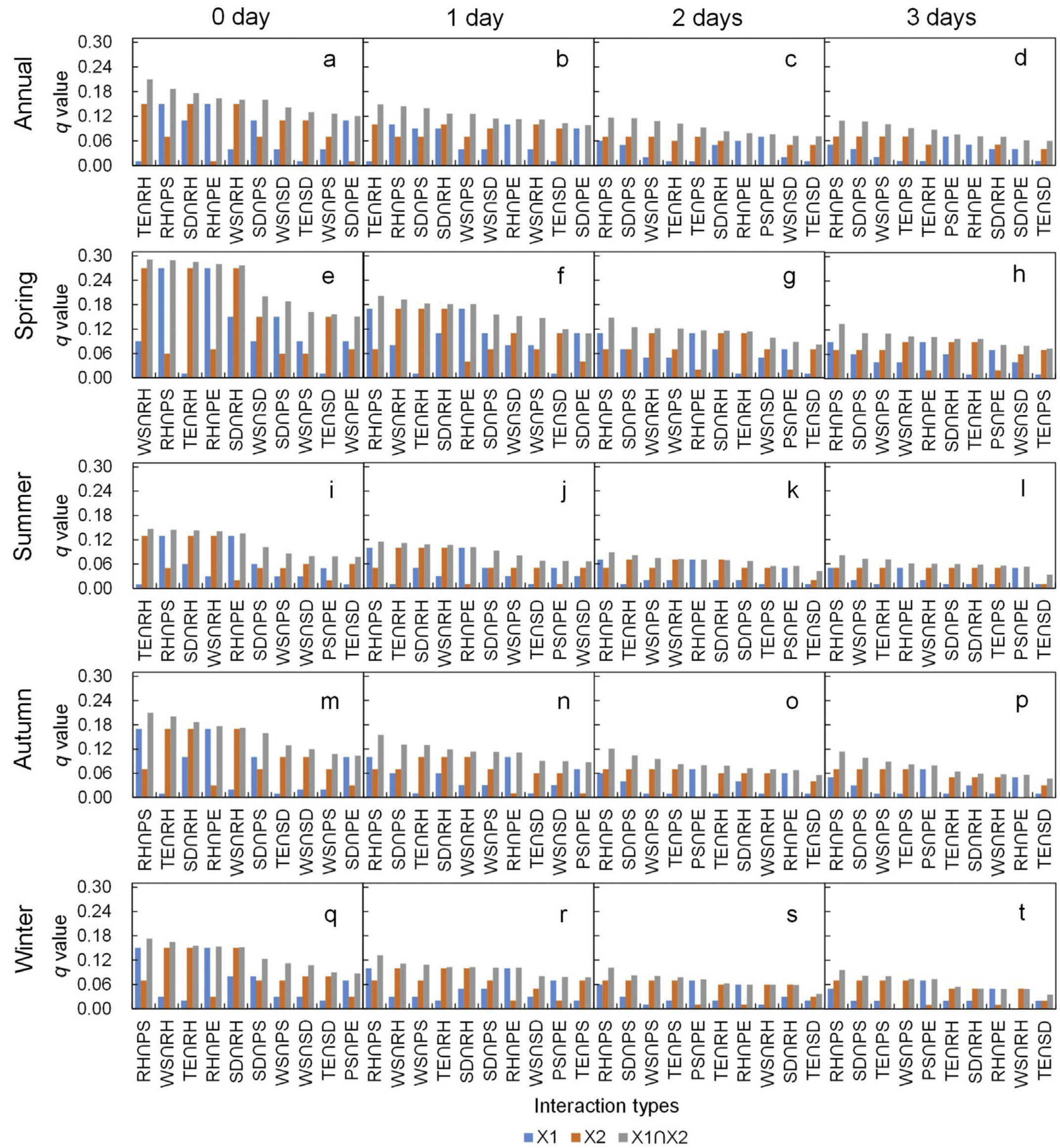

Fig. 10. Interactive hysteretic effects of meteorological conditions on $PM_{2.5}/PM_{10}$ ratio in China. The x-axis label X1∩X2 denotes q values of X1 (blue), X2 (yellow), and the interaction between X1 and X2 (grey). (For interpretation of the references to color in this figure legend, the reader is referred to the Web version of this article.)

meteorological conditions on PM concentrations and $PM_{2.5}/PM_{10}$ ratios with stable anthropogenic emissions within a specific time and region.

Significant regional and seasonal variations in the hysteretic effects of meteorological factors on PM were observed. In general, TE was the primary hysteretic factor; it showed negative impacts on the $PM_{2.5}$ concentration (Fig. 3) at the national scale, especially in regions of EC, MUYR, MYR, NC, NE, and UYR, throughout the whole year. The higher surface temperature could stimulate the diffusion capability of the troposphere and elevate the height of the planetary boundary layer (PBL) (Wallace and Kanaroglou, 2009; Li et al., 2019b), which resulted in the lower $PM_{2.5}$ concentrations by diffusion and dilution. In regions of MUPR and SC, PE was the main lagged factor and showed negative effects on $PM_{2.5}$ concentrations. This was mainly because higher precipitation in these regions had the strong ability to scavenge particulate matter of the next few days by wet deposition (Guan et al., 2017; Cai et al., 2019; Li et al., 2019a, 2019b). However, the primary hysteretic factor of $PM_{2.5}$ was WS which is inversely correlated to PM in winter. This is due to the inter-regional transport of PM by strong winds, which is consistent with previous studies (Hien et al., 2002; Huang et al., 2015) and is presumably because the East Asian winter monsoon transports PM from northern to southern China within two to three days (Wang et al., 2019). Generally, SD was a dominant hysteretic factor of $PM_{2.5}/PM_{10}$ ratios, and $PM_{2.5}/PM_{10}$ had negative correlations with SD (Fig. 3). This is because more sunshine can enhance vertical temperature gradient, facilitating the dispersion of fine PM (Liu et al., 2018). In addition, long SD can accelerate the formation of secondary PM, especially PM_{10}, thus promoting the decline of $PM_{2.5}/PM_{10}$ (Li et al., 2019b).

PE was the dominant lagged factor and had negative correlation on PM_{10} concentrations, especially in the autumn in northern China. This is also because PE can scavenge particulate matter through wet depositions (Lin et al., 2015; Li et al., 2017a, 2017b; Wang et al., 2016a). Moreover, PE can also retard the release of natural and fugitive dust into the atmosphere by increasing soil moisture (Li et al., 2019b). Although the correlation coefficient between PM_{10} concentrations and meteorological factors showed

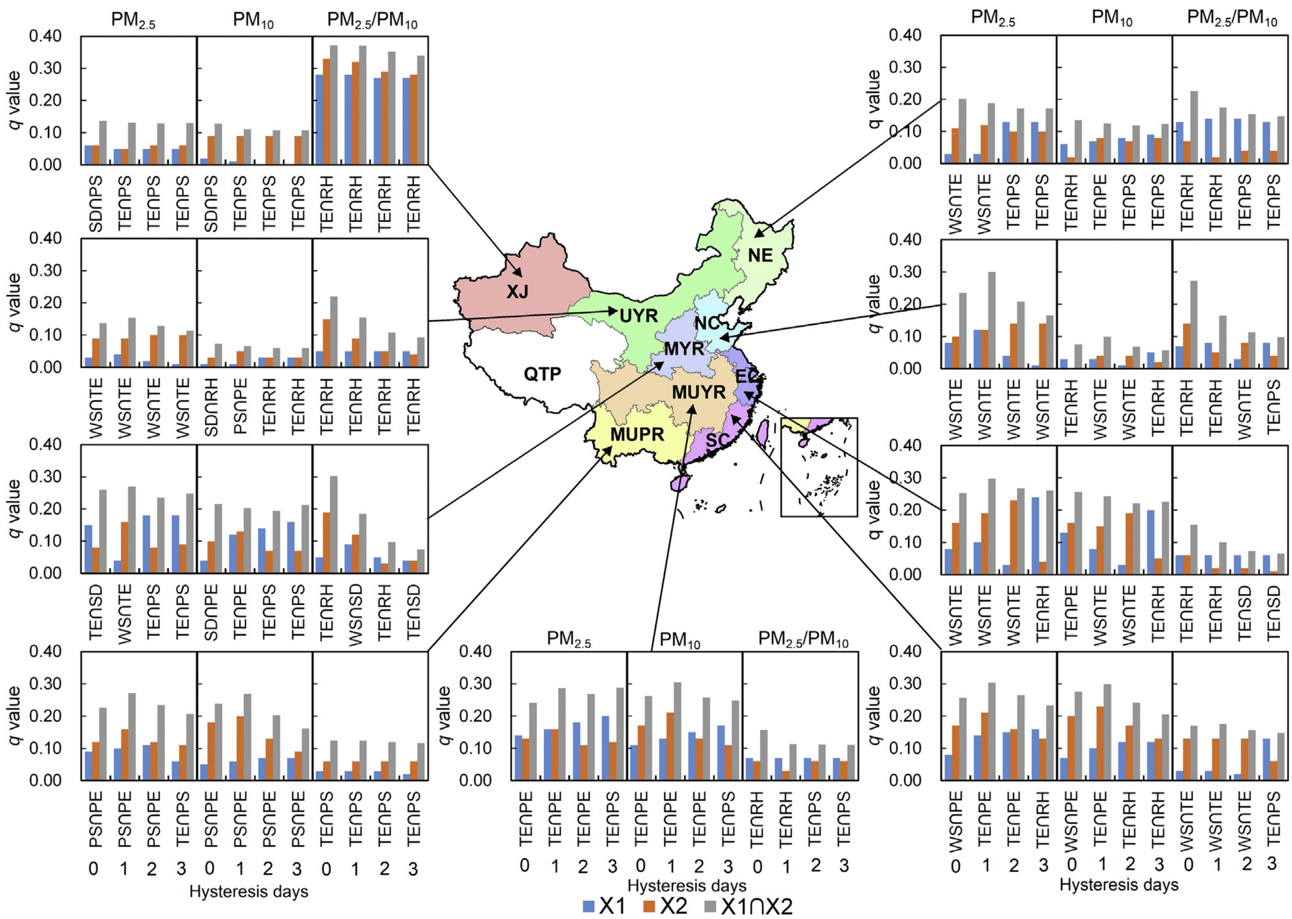

Fig. 11. Regional hysteretic effects of interactions between meteorological factors on PM at the annual time scale in China.

that RH and TE had stronger negative effects than other factors (Fig. 3), PE was the dominant hysteretic factor. This collinearity among influencing factors indicates that the relative importance of meteorological factors in the formation of PM cannot be assessed based on the correlation coefficient alone. RH was the dominant hysteretic factor and exhibited positively correlated with $PM_{2.5}/PM_{10}$ ratios, especially in spring and regions of MYR, NC, UYR, and XJ. This is due to RH can stimulate the secondary $PM_{2.5}$ conversion rate and enhance the hygroscopic growth rate when RH < 70%, while high RH (>70%) can reduce PM concentrations by wet deposition, especially PM_{10} (Lou et al., 2017).

Interactions between meteorological factors showed significantly enhanced effects on PM concentrations or $PM_{2.5}/PM_{10}$ ratios compared to a single factor. WS∩TE and TE∩PE showed strongest effects on $PM_{2.5}$ concentrations on days L1 and L2, respectively. Air temperature could change the pressure gradient, generating strong winds when the pressure gradient is steep. This can stimulate the diffusion of $PM_{2.5}$ and have significant impacts on next day's $PM_{2.5}$ concentrations. Generally, precipitation and temperature are negatively and positively correlated to each other in summer and winter, respectively, over land in the northern hemisphere (Trenberth and Shea, 2005). There is a close relationship between air temperature and precipitation and they affect each other (Trenberth and Shea, 2005). Changes in air temperature and precipitation will directly affect the formation process of secondary PM and the dry/wet PM deposition, and thus change PM concentrations. Temperature directly influences relative humidity, which in turn influences the potential for precipitation; this explain the primary effects of the interaction between TE and RH on the next day's $PM_{2.5}/PM_{10}$ ratio.

4.2. Model validation

In order to verify the validity of the results of this study, we selected MYR region in winter as an example to develop regression prediction models for $PM_{2.5}$. Factors of SD, RH, and WS and of WS, RH, and SD were selected as independent variables on L0 and L1, respectively. Fig. 12 shows regression models for MYR region and their performance in one city of Zhengzhou, Henan province with severe PM pollution in winter. We can see that the prediction models can well simulate $PM_{2.5}$ concentrations on both days of L0 and L1. However, models on days of L2 and L3 were not shown here due to its poor performance due to the lower q values. This indicated that the q values of hysteretic factors can impact the performance of prediction models. The larger the q value, the better the model performance, and vice versa. Therefore, this study can be very helpful to select dominant impacting factors and develop PM prediction models.

5. Conclusions

This study found that there were large regional and seasonal variations in the hysteretic effects of meteorological conditions and their interactions on PM concentrations or $PM_{2.5}/PM_{10}$ ratios. At the nationwide scale, PE, RH, and TE were the major hysteretic factors influencing $PM_{2.5}$ and PM_{10} concentrations, and $PM_{2.5}/PM_{10}$ ratios

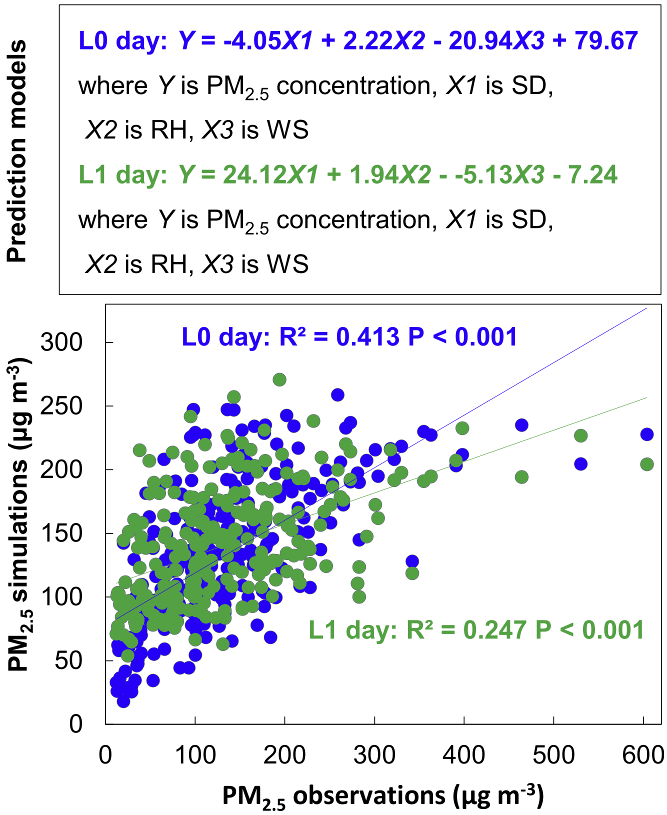

Fig. 12. Simulation performance of regression models based on the dominant hysteretic factors that were detected in MYR region in winter (taking Zhengzhou, Henan Province as an example). Blue and green color denote days of L0 and L1, respectively. (For interpretation of the references to color in this figure legend, the reader is referred to the Web version of this article.)

throughout the whole year. The dominant hysteretic factor of PM concentrations was PE in autumn, but was WS in winter. In regions of MUPR and SC, PE was the primary lagged factor of the $PM_{2.5}$ concentration. For $PM_{2.5}/PM_{10}$ ratios, TE was the main hysteretic factor in regions of SC and NE.

These findings regarding the hysteretic effects of meteorological conditions and their interactions on PM in China can contribute to the development of scientific control strategies in severely polluted areas. For example, knowing that RH is the dominant impacting factor and positively correlated to next day's $PM_{2.5}$ concentration, we can take measures, such as traffic restriction, increasing the frequency of watering to suppress dust on construction sites and roads, and industrial enterprises implement off-peak production or stop production. This can reduce PM and its precursor emissions such as sulfur dioxide, ammonia, nitrogen oxide, and volatile organic compounds in MYR, thereby improving the air quality. Equally importantly, these findings provide valuable information for improving the performance of pollution prediction models.

CRediT authorship contribution statement

Tuanhui Wang: Software, Writing - original draft. **Hongquan Song:** Conceptualization, Supervision, Writing - review & editing, Funding acquisition. **Feng Wang:** Software, Visualization, Data curation. **Shiyan Zhai:** Software, Visualization, Data curation. **Zhigang Han:** Data curation, Investigation. **Dong Wang:** Data curation, Investigation. **Xiaoyang Li:** Data curation, Investigation. **Haipeng Zhao:** Investigation. **Rui Ma:** Validation, Visualization. **Guangli Zhang:** Validation, Visualization.

Declaration of competing interest

The authors declare that they have no known competing financial interests or personal relationships that could have appeared to influence the work reported in this paper.

Acknowledgements

This study was financially supported by the National Natural Science Foundation of China, China (41401107, 41871316) and the Basic Frontier and Technology Research Project of Henan Province, China (162300410132).

Appendix A. Supplementary data

Supplementary data to this article can be found online at https://doi.org/10.1016/j.jclepro.2020.122926.

References

Aunan, K., Ma, Q., Lund, M.T., Wang, S., 2018. Population-weighted exposure to PM2.5 pollution in China: an integrated approach. Environ. Int. 120, 111–120. https://doi.org/10.1016/j.envint.2018.07.042.

Barmpadimos, I., Hueglin, C., Keller, J., Henne, S., Prévôt, A.S.H., 2011. Influence of meteorology on PM10 trends and variability in Switzerland from 1991 to 2008. Atmos. Chem. Phys. 11 (4), 1813–1835. https://doi.org/10.5194/acp-11-1813-2011.

Cai, M., Xin, Z., Yu, X., 2019. Particulate matter transported from urban greening plants during precipitation events in Beijing, China. Environ. Pollut. 252, 1648–1658. https://doi.org/10.1016/j.envpol.2019.06.119.

Chen, G., Li, S., Knibbs, L.D., Hamm, N.A., Cao, W., Li, T., Guo, Y., 2018a. A machine learning method to estimate PM2.5 concentrations across China with remote sensing, meteorological and land use information. Sci. Total Environ. 636, 52–60. https://doi.org/10.1016/j.scitotenv.2018.04.251.

Chen, T., He, J., Lu, X., She, J., Guan, Z., 2016. Spatial and temporal variations of PM2.5 and its relation to meteorological factors in the urban area of Nanjing, China. Int. J. Environ. Res. Publ. Health 13 (9), 921. https://doi.org/10.3390/ijerph13090921.

Chen, Z., Cai, J., Gao, B., Xu, B., Dai, S., He, B., Xie, X., 2017. Detecting the causality influence of individual meteorological factors on local PM2.5 concentration in the Jing-Jin-Ji region. Sci. Rep. UK 7, 40735. https://doi.org/10.1038/srep40735.

Chen, Z.Y., Zhang, T.H., Zhang, R., Zhu, Z.M., Ou, C.Q., Guo, Y., 2018b. Estimating PM2.5 concentrations based on non-linear exposure-lag-response associations with aerosol optical depth and meteorological measures. Atmos. Environ. 173, 30–37. https://doi.org/10.1016/j.atmosenv.2017.10.055.

Gu, Y., Liou, K.N., Chen, W., Liao, H., 2010. Direct climate effect of black carbon in China and its impact on dust storms. J. Geophys. Res. Atmos. 115, D00K14. https://doi.org/10.1029/2009JD013427.

Guan, Q., Cai, A., Wang, F., Yang, L., Xu, C., Liu, Z., 2017. Spatio-temporal variability of particulate matter in the key part of Gansu Province, Western China. Environ. Pollut. 230, 189–198. https://doi.org/10.1016/j.envpol.2017.06.045.

Guan, Y., Kang, L., Wang, Y., Zhang, N.N., Ju, M.T., 2019. Health loss attributed to PM2.5 pollution in China's cities: economic impact, annual change and reduction potential. J. Clean. Prod. 217, 284–294. https://doi.org/10.1016/j.jclepro.2019.01.284.

Guo, L.C., Zhang, Y., Lin, H., Zeng, W., Liu, T., Xiao, J., Ma, W., 2016. The washout effects of rainfall on atmospheric particulate pollution in two Chinese cities. Environ. Pollut. 215, 195–202. https://doi.org/10.1016/j.envpol.2016.05.003.

He, J., Gong, S., Yu, Y., Yu, L., Wu, L., Mao, H., Li, R., 2017. Air pollution characteristics and their relation to meteorological conditions during 2014–2015 in major Chinese cities. Environ. Pollut. 223, 484–496. https://doi.org/10.1016/j.envpol.2017.01.050.

Hien, P.D., Bac, V.T., Tham, H.C., Nhan, D.D., Vinh, L.D., 2002. Influence of meteorological conditions on PM2.5 and PM2.5–10 concentrations during the monsoon season in Hanoi. Vietnam. Atmos. Environ. 36 (21), 3473–3484. https://doi.org/10.1016/s1352-2310(02)00295-9.

Hong, C., Zhang, Q., Zhang, Y., Davis, S.J., Tong, D., Zheng, Y., Liu, Z., Guan, D., He, K., Schellnhuber, H.J., 2019. Impacts of climate change on future air quality and human health in China. Proc. Natl. Acad. Sci. USA 116 (35), 17193–17200. https://doi.org/10.1073/pnas.1812881116.

Huang, X., Wang, D., Han, P., Wang, W., Li, Q., Zhang, X., Ma, M., Li, B., Han, S., 2020. Spatial patterns in baseflow mean response time across a watershed in the Loess Plateau: Linkage with Land-use types. Forest Sci. 66 (3), 382–391. https://doi.org/10.1093/forsci/fxz084.

Huang, D., Xu, Y., Peng, P., Zhang, H., Lan, J., 2009. Chemical composition and seasonal variation of acid deposition in Guangzhou, South China: comparison with precipitation in other major Chinese cities. Environ. Pollut. 157 (1), 35–41. https://doi.org/10.1016/J.ENVPOL.2008.08.001.

Huang, F., Li, X., Wang, C., Xu, Q., Wang, W., Luo, Y., Cao, K., 2015. PM2.5

spatiotemporal variations and the relationship with meteorological factors during 2013-2014 in Beijing, China. PloS One 10 (11), e0141642. https://doi.org/10.1371/journal.pone.0141642.

Ito, K., Thurston, G.D., Silverman, R.A., 2007. Characterization of PM2.5, gaseous pollutants, and meteorological interactions in the context of time-series health effects models. J. Expo. Sci. Environ. Epidemiol. 17 (S2), S45–S60. https://doi.org/10.1038/sj.jes.7500627.

Jing, Z., Liu, P., Wang, T., Song, H., Lee, J., Xu, T., Xing, Y., 2020. Effects of meteorological factors and anthropogenic precursors on $PM_{2.5}$ concentrations in cities in China. Sustainability 12, 3550. https://doi.org/10.3390/SU12093550.

Khan, R., Konishi, S., Ng, C.F.S., Umezaki, M., Kabir, A.F., Tasmin, S., Watanabe, C., 2019. Association between short-term exposure to fine particulate matter and daily emergency room visits at a cardiovascular hospital in Dhaka, Bangladesh. Sci. Total Environ. 646, 1030–1036. https://doi.org/10.1016/j.scitotenv.2018.07.288.

Kliengchuay, W., Cooper Meeyai, A., Worakhunpiset, S., Tantrakarnapa, K., 2018. Relationships between meteorological parameters and particulate matter in mae Hong son province, Thailand. Int. J. Environ. Res. Publ. Health 15 (12), 2801. https://doi.org/10.3390/ijerph15122801.

Li, R., Wang, Z., Cui, L., Fu, H., Zhang, L., Kong, L., Chen, J., 2019a. Air pollution characteristics in China during 2015–2016: spatiotemporal variations and key meteorological factors. Sci. Total Environ. 648, 902–915. https://doi.org/10.1016/j.scitotenv.2018.08.181.

Li, X., Chen, X., Yuan, X., Zeng, G., León, T., Liang, J., Yuan, X., 2017a. Characteristics of particulate pollution (PM2.5 and PM10) and their spacescale-dependent relationships with meteorological elements in China. Sustainability 9 (12), 2330. https://doi.org/10.3390/su9122330.

Li, X., Ma, Y., Wang, Y., Liu, N., Hong, Y., 2017b. Temporal and spatial analyses of particulate matter (PM_{10} and $PM_{2.5}$) and its relationship with meteorological parameters over an urban city in northeast China. Atmos. Res. 198, 185–193. https://doi.org/10.1016/j.atmosres.2017.08.023.

Li, X., Song, H., Zhai, S., Lu, S., Kong, Y., Xia, H., Zhao, H., 2019b. Particulate matter pollution in Chinese cities: areal-temporal variations and their relationships with meteorological conditions (2015–2017). Environ. Pollut. 246, 11–18. https://doi.org/10.1016/j.envpol.2018.11.103.

Li, X., Zhang, Q., Zhang, Y., Zheng, B., Wang, K., Chen, Y., Wallington, T.J., Han, W., Shen, W., Zhang, X., He, K., 2015a. Source contributions of urban $PM_{2.5}$ in the Beijing-Tianjin-Hebei region: changes between 2006 and 2013 and relative impacts of emissions and meteorology. Atmos. Environ. 123, 229–239. https://doi.org/10.1016/j.atmosenv.2015.10.048.

Li, Y., Chen, Q., Zhao, H., Wang, L., Tao, R., 2015b. Variations in PM10, PM2.5 and PM1.0 in an urban area of the Sichuan Basin and their relation to meteorological factors. Atmosphere 6 (1), 150–163. https://doi.org/10.3390/atmos6010150.

Lin, G., Fu, J., Jiang, D., Wang, J., Wang, Q., Dong, D., 2015. Spatial variation of the relationship between $PM_{2.5}$ concentrations and meteorological parameters in China. BioMed Res. Int. 2015 (21), 259–265. https://doi.org/10.1155/2015/684618.

Liu, X., Ouyang, W., Shu, Y., Tian, Y., Feng, Y., Zhang, T., Chen, W., 2019. Incorporating bioaccessibility into health risk assessment of heavy metals in particulate matter originated from different sources of atmospheric pollution. Environ. Pollut. 254, 113113. https://doi.org/10.1016/j.envpol.2019.113113.

Liu, Y., Wu, J., Yu, D., Hao, R., 2018. Understanding the patterns and drivers of air pollution on multiple time scales: the case of Northern China. Environ. Manag. 61 (6), 1048–1061. https://doi.org/10.1007/s00267-018-1026-5.

Lou, C., Liu, H., Li, Y., Peng, Y., Wang, J., Dai, L., 2017. Relationships of relative humidity with $PM_{2.5}$ and PM_{10} in the Yangtze River delta, China. Environ. Monit. Assess. 189 (11), 582. https://doi.org/10.1007/s10661-017-6281-z.

Miao, Y., Liu, S., Guo, J., Yan, Y., Huang, S., Zhang, G., Lou, M., 2018. Impacts of meteorological conditions on wintertime PM2.5 pollution in Taiyuan, North China. Environ. Sci. Pollut. Res. 25 (22), 21855–21866. https://doi.org/10.1007/s11356-018-2327-1.

Miranda, R.M.D., Andrade, M.D.F., Fornaro, A., Astolfo, R., Andre, P.A.D., Saldiva, P., 2012. Urban air pollution: a representative survey of $PM_{2.5}$ mass concentrations in six brazilian cities. Air Qual. Atmos. Health 5 (1), 63–77. https://doi.org/10.1007/s11869-010-0124-1.

Phosri, A., Ueda, K., Phung, V.L.H., Tawatsupa, B., Honda, A., Takano, H., 2019. Effects of ambient air pollution on daily hospital admissions for respiratory and cardiovascular diseases in Bangkok, Thailand. Sci. Total Environ. 651, 1144–1153. https://doi.org/10.1016/j.scitotenv.2018.09.183.

Shen, W., Ren, H., Jenerette, G.D., Hui, D., Ren, H., 2013. Atmospheric deposition and canopy exchange of anions and cations in two plantation forests under acid rain influence. Atmos. Environ. 64, 242–250. https://doi.org/10.1016/J.ATMOSENV.2012.10.015.

Song, H., Wang, K., Zhang, Y., Hong, C., Zhou, S., 2017. Simulation and evaluation of dust emissions with WRF-Chem (v3.7.1) and its relationship to the changing climate over East Asia from 1980 to 2015. Atmos. Environ. 167, 511–522. https://doi.org/10.1016/j.atmosenv.2017.08.051.

Trenberth, K.E., Shea, D.J., 2005. Relationships between precipitation and surface temperature. Geophys. Res. Lett. 32 (14), L14703. https://doi.org/10.1029/2005GL022760.

Wallace, J., Kanaroglou, P., 2009. The effect of temperature inversions on ground-level nitrogen dioxide (NO_2) and fine particulate matter ($PM_{2.5}$) using temperature profiles from the Atmospheric Infrared Sounder (AIRS). Sci. Total Environ. 407 (18), 5085–5095. https://doi.org/10.1016/j.scitotenv.2009.05.050.

Wang, C., An, X., Zhang, P., Sun, Z., Cui, M., Ma, L., 2019. Comparing the impact of strong and weak East Asian winter monsoon on $PM_{2.5}$ concentration in Beijing. Atmos 215, 165–177. https://doi.org/10.1016/j.atmosres.2018.08.022.

Wang, H.L., Qiao, L.P., Lou, S.R., Zhou, M., Ding, A.J., Huang, H.Y., Chen, J.M., Wang, Q., Tao, S.K., Chen, C.H., Li, L., Huang, C., 2016a. Chemical composition of PM2.5 and meteorological impact among three years in urban Shanghai, China. J. Clean. Prod. 112 (2), 1302–1311. https://doi.org/10.1016/j.jclepro.2015.04.099.

Wang, J., Ogawa, S., 2015. Effects of meteorological conditions on PM2.5 concentrations in Nagasaki, Japan. Int. J. Environ. Res. Publ. Health 12 (8), 9089–9101. https://doi.org/10.3390/ijerph120809089.

Wang, J.F., Li, X.H., Christakos, G., Liao, Y.L., Zhang, T., Gu, X., Zheng, X.Y., 2010. Geographical detectors-based health risk assessment and its application in the neural tube defects study of the Heshun Region, China. Int. J. Geogr. Inf. Sci. 24 (1), 107–127. https://doi.org/10.1080/13658810802443457.

Wang, J.F., Zhang, T.L., Fu, B.J., 2016b. A measure of spatial stratified heterogeneity. Ecol. Indicat. 67, 250–256. https://doi.org/10.1016/j.ecolind.2016.02.052.

Wang, S., Liu, X., Yang, X., Zou, B., Wang, J., 2018. Spatial variations of PM2.5 in Chinese cities for the joint impacts of human activities and natural conditions: a global and local regression perspective. J. Clean. Prod. 203, 143–152. https://doi.org/10.1016/j.jclepro.2018.08.249.

Wang, Y.Q., Zhang, X.Y., Sun, J.Y., Zhang, X.C., Che, H.Z., Li, Y., 2015. Spatial and temporal variations of the concentrations of PM10, PM2.5 and PM1 in China. Atmos. Chem. Phys. 15 (23), 13585–13598. https://doi.org/10.5194/acp-15-13585-2015.

Xie, J., Jin, L., Cui, J., Luo, X., Li, J., Zhang, G., Li, X., 2020. Health risk-oriented source apportionment of PM2.5-associated trace metals. Environ. Pollut. 262, 114655. https://doi.org/10.1016/j.envpol.2020.114655.

Xue, W., Zhang, J., Zhong, C., Ji, D., Huang, W., 2019. Satellite-derived spatiotemporal PM2.5 concentrations and variations from 2006 to 2017 in China. Sci. Total Environ. https://doi.org/10.1016/j.scitotenv.2019.134577.

Yang, D., Wang, X., Xu, J., Xu, C., Lu, D., Ye, C., Bai, L., 2018. Quantifying the influence of natural and socioeconomic factors and their interactive impact on PM2.5 pollution in China. Environ. Pollut. 241, 475–483. https://doi.org/10.1016/j.envpol.2018.05.043.

Yin, Q., Wang, J., Hu, M., Wong, H., 2016. Estimation of daily PM2.5 concentration and its relationship with meteorological conditions in Beijing. J. Environ. Sci. China 48, 161–168. https://doi.org/10.1016/j.jes.2016.03.024.

Zhang, F., Chen, J., Qiu, T., Yin, L., Chen, X., Yu, J., 2013. Pollution characteristics of PM2.5 during a typical haze episode in Xiamen, China. Atmos. Clim. Sci. 3 (4), 427. https://doi.org/10.4236/acs.2013.34044.

Zhang, W., Wang, H., Zhang, X., Peng, Y., Zhong, J., Wang, Y., Zhao, Y., 2020. Evaluating the contributions of changed meteorological conditions and emission to substantial reductions of $PM_{2.5}$ concentration from winter 2016 to 2017 in Central and Eastern China. Sci. Total Environ. 136892. https://doi.org/10.1016/j.scitotenv.2020.136892.

Zhang, X., Chen, L., Yuan, R., 2019. Effect of natural and anthropic factors on the spatiotemporal pattern of haze pollution control of China. J. Clean. Prod. 119531. https://doi.org/10.1016/j.jclepro.2019.119531.

Zhu, G., Hu, W., Liu, Y., Cao, J., Ma, Z., Deng, Y., Sabel, C., Wang, H., 2019. Health burdens of ambient PM2.5 pollution across Chinese cities during 2006–2015. J. Environ. Manag. 243, 250–256. https://doi.org/10.1016/j.jenvman.2019.04.119.